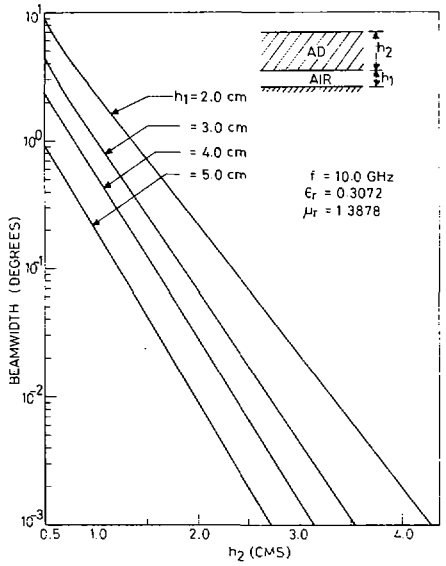

Fig. 6. Variation of beamwidth with h_2 for various values of h_1.

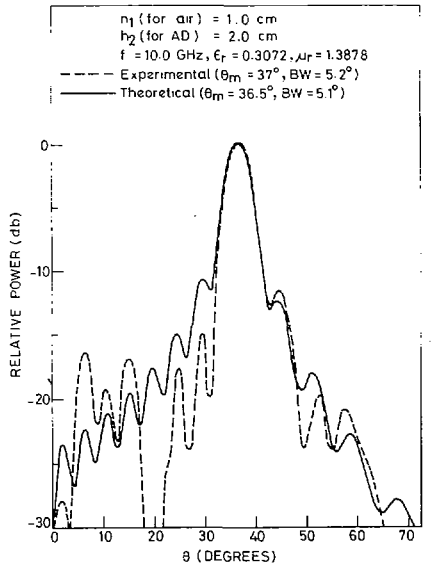

Fig. 7. Comparison of experimental and theoretical radiation patterns at 10 GHz (for bidirectional excitation, L = 40 cm).

height h_1 = 1 cm and effective AD height h_2 = 2 cm. In the z direction there are 80 columns of wire separated by a distance of 1 cm. The structure is excited by feeding power to the central wire in the first row of wires. The experimental setup and the procedure for the measurement of the radiation pattern is the same one used in [1] except that the receiving horn is replaced by a parabolic dish.

An experimental radiation pattern measured at 10 GHz is shown in Fig. 7. The theoretical pattern calculated from [1, eq. (11)] for this case is also shown in this figure. It is noted that the measured beamwidth is 5.2° and the theoretical (for TE_{00} mode) is 5.1°. The position of the beam agrees within 0.5°. The two side lobe levels in the experimental radiation pattern are 15 dB and 11.5 dB below the peak whereas corresponding theoretical values are 11 dB and 12.5 dB, respectively. The experimental radiation pattern shows another peak at about 7° which is due to the propagation of the second-order mode (m = 1). The theoretical position of this second peak is 9°. The overall agreement between the theoretical and the experimental radiation patterns is good.

V. Comparison Between Dielectric–AD Slab and AD Slab Antennas

As was mentioned earlier a dielectric–AD antenna structure has a significant feature of controlling beam position and beamwidth independently. For a given dielectric layer height (and hence θ_m), the attenuation along the length of the structure may be controlled by adjusting the thickness of the AD. Thus the amplitude distribution can be adjusted without disturbing phase distribution. This feature may be utilized in constructing an antenna with amplitude distribution tailored to reduce side lobe levels. This characteristic does not exist for grounded AD slabs [1].

Another feature of the dielectric–AD antenna is that it requires a smaller volume of AD (and also the overall volume is smaller) when compared to an AD antenna of similar characteristics. This can be seen from the following example. At 10 GHz an AD antenna with θ_m = 35.5° and BW = 4.8° [1] requires h = 5 cm and L = 80 cm (bidirectional excitation). For a dielectric–AD antenna similar performance (θ_m = 37°, BW = 5.1°) is obtained for h_1 = 1 cm, h_2 = 2 cm, and L = 80 cm (bidirectional excitation) when the same AD is used.

References

[1] I. J. Bahl and K. C. Gupta, "A leaky-wave antenna using an artificial dielectric medium," *IEEE Trans. Antennas Propagat.* (Commun.), vol. AP-22, pp. 119–122, Jan. 1974.
[2] J. H. Harris, "Leaky-wave beams of multiply layered plasma media," *Radio Sci.*, vol. 3, p. 181, Feb. 1968.
[3] R. E. Collin, "Analytical solution for a leaky-wave antenna," *IRE Trans. Antennas Propagat.*, vol. AP-10, pp. 561–565, Sept. 1962.
[4] R. E. Collin and F. J. Zucker, *Antenna Theory, Part II.* New York: McGraw-Hill, 1969, p. 257,

Design of Line-Source Antennas for Sum Patterns with Sidelobes of Individually Arbitrary Heights

ROBERT S. ELLIOTT, FELLOW, IEEE

Abstract—**A design method is presented for the determination of continuous line sources which will yield sum patterns consisting of a narrow main beam and sidelobes whose individual heights can be adjusted to any arbitrary specification. The method is based on a generalized Taylor pattern which is perturbed in successive iterations until the desired pattern results. For practical cases the convergence is rapid, and an economical computer program of general applicability has been written which will terminate when the desired pattern has been achieved within a specified tolerance, at which point a final pattern and aperture distribution are printed out. The theory is illustrated by several cases of practical interest.**

Manuscript received April 16, 1975; revised August 17, 1975. This work was supported by the Hughes Aircraft Company.
The author is with the Department of Electrical Sciences, University of California, Los Angeles, CA, and is also a consultant to the Hughes Aircraft Company, Canoga Park, CA 91304.

Introduction

Two widely used design techniques for the synthesis of line source distributions which yield antenna radiation patterns with a narrow main beam and *symmetrical* sidelobes are due to Dolph [1] and Taylor [2]. Dolph's method is applicable to discrete arrays and results in patterns in which all the sidelobes are at a common height; Dolph has demonstrated that his approach, which uses a transformation of Chebyshev polynomials, gives the narrowest beamwidth for a specified sidelobe level. Taylor's method deals with continuous aperture distributions which correspond to a radiation pattern with a narrow main beam and symmetric sidelobes; a specified number of these sidelobes on each side of the main beam (extending to the limits of the visible region, if desired) can be designed to be at essentially the same level, with the farther out sidelobes decaying in height. The Taylor pattern is representable as a canonical product of factors whose roots are the zeros of the pattern. Computer programs which will yield Dolph or Taylor aperture distributions for patterns with prescribed beamwidths and sidelobe levels are simple to write and widely used by antenna designers.

Many applications exist in which it is not necessary (nor in some cases desirable) to have uniformly low sidelobes, and it is well known that some beam-narrowing (with a concomitant rise in gain) will result if some of the sidelobes are permitted to rise. Recently, some work has been reported [3] which indicates how a line source may be synthesized to yield *asymmetric* sidelobes, that is, near-in sidelobes all of essentially a common height on one side of the main beam, and near-in sidelobes of a common but different height on the other side of the main beam.

The general problem of designing a line source to yield a pattern with an arbitrary sidelobe level envelope has been studied by Hyneman [4] and Stutzman [5]. Starting with a suitably modified Taylor pattern, Hyneman developed a perturbation procedure based on the log derivative of the envelope function. This led to computable shifts in the pattern zeros which caused an approximation to the requisite pattern. Stutzman used an iterative sampling method to make the sidelobe peaks conform to a specified shape within a given tolerance.

The present paper also pertains to the general problem of arbitrary control of the levels of individual sidelobes, and uses a Taylor pattern as the starting point. However, the perturbation procedure is fundamentally different from those used by Hyneman and Stutzman, and employs a computer program which is felt to be more economical. For all practical applications which have been investigated, convergence to the desired pattern has been obtained to any degree of accuracy specified.

Analysis

A conventional Taylor pattern [2, p. 22] is expressible in the form

$$F_0(z) = \frac{\sin \pi z}{\pi z} \frac{\prod_{n=1}^{\bar{n}-1} \left(1 - \frac{z^2}{z_n^2}\right)}{\prod_{n=1}^{\bar{n}-1} \left(1 - \frac{z^2}{n^2}\right)} \tag{1}$$

in which $z = (2a/\lambda) \cos \theta$, with $2a/\lambda$ the aperture extent in wavelengths, and with θ the angle measured from endfire. The roots z_n are given by

$$z_n = \pm \sigma \sqrt{A^2 + (n - \tfrac{1}{2})^2} \tag{2}$$

in which

$$\sigma = \frac{\bar{n}}{\sqrt{A^2 + (\bar{n} - \tfrac{1}{2})^2}} \tag{3}$$

wherein $\cosh \pi A$ is the voltage sidelobe level. $\bar{n}$ is a transition integer such that there are $\bar{n} - 1$ near-in sidelobes on each side of the main beam, all of essentially the same height, whereas the $\bar{n}$th lobe and all others further out decay in height as z^{-1}.

A generalization of (1), appropriate for asymmetrical patterns [3], is

$$F_0(z) = \frac{\sin \pi z}{\pi z} \frac{\prod_{n=1}^{\bar{n}_R-1} \left(1 - \frac{z}{R_n^0}\right) \prod_{n=1}^{\bar{n}_L-1} \left(1 - \frac{z}{L_n^0}\right)}{\prod_{n=1}^{\bar{n}_R-1} \left(1 - \frac{z}{n}\right) \prod_{n=1}^{\bar{n}_L-1} \left(1 + \frac{z}{n}\right)} \tag{4}$$

in which

$$R_n^0 = \sigma_R \sqrt{A_R^2 + (n - \tfrac{1}{2})^2} \qquad L_n^0 = -\sigma_L \sqrt{A_L^2 + (n - \tfrac{1}{2})^2}$$

with

$$\sigma_R = \frac{\bar{n}_R}{\sqrt{A_R^2 + (\bar{n}_R - \tfrac{1}{2})^2}} \qquad \sigma_L = \frac{n}{\sqrt{A_L^2 + (\bar{n}_L - \tfrac{1}{2})^2}} \tag{6}$$

and with $\cosh \pi A_R$, $\cosh \pi A_L$ the voltage sidelobe levels on the right and left sides of the main beam; $\bar{n}_R$ and $\bar{n}_L$ are the transition numbers.

In the perturbation procedure to be developed, if the desired pattern were symmetrical, one would start from (1), whereas if it were asymmetrical, one would start from (4). This point will be elaborated later on in the development. However, since (1) may be viewed as a special case of (4), the theory will be based on (4) as a starting point.

The pattern represented by (4) can be modified by shifting the zeros to new potisions R_n, L_n, given by

$$R_n = R_n^0 + r_n \tag{7}$$

$$L_n = L_n^0 + l_n \tag{8}$$

in which r_n and l_n are the perturbations. The new pattern will be

$$F(z) = \frac{\sin \pi z}{\pi z} \frac{\prod_{n=1}^{\bar{n}_R-1} \left(1 - \frac{z}{R_n}\right) \prod_{n=1}^{\bar{n}_L-1} \left(1 - \frac{z}{L_n}\right)}{\prod_{n=1}^{\bar{n}_R-1} \left(1 - \frac{z}{n}\right) \prod_{n=1}^{\bar{n}_L-1} \left(1 - \frac{z}{n}\right)} \tag{9}$$

and the goal is to find those values of r_n and l_n which will convert the starting pattern $F_0(z)$ into the desired pattern $F(z)$.

Since

$$\begin{aligned} 1 - \frac{z}{R_n} &= 1 - z(R_n^0 + r_n)^{-1} \\ &\cong 1 - z[(R_n^0)^{-1} - r_n(R_n^0)^{-2}] \\ &\cong \left(1 - \frac{z}{R_n^0}\right) + \frac{z r_n}{(R_n^0)^2} \end{aligned}$$

it follows that, to first order,

$$\prod_{n=1}^{\bar{n}_R-1} \left(1 - \frac{z}{R_n}\right) = \left[\prod_{n=1}^{\bar{n}_R-1} \left(1 - \frac{z}{R_n^0}\right)\right] \cdot \left[1 + \sum_{n=1}^{\bar{n}_R-1} \frac{\left(\frac{z}{R_n^0}\right)\left(\frac{r_n}{R_n^0}\right)}{\left(1 - \frac{z}{R_n^0}\right)}\right]. \tag{10}$$

When (10) and the equivalent expression for the left-hand product are inserted in (4), one obtains the first-order relation

$$F(z) = F_0(z)\left[1 + \sum_{n=1}^{\bar{n}_R-1} \frac{\left(\frac{z}{R_n^0}\right)\left(\frac{r_n}{R_n^0}\right)}{\left(1 - \frac{z}{R_n^0}\right)} + \sum_{n=1}^{\bar{n}_L-1} \frac{\left(\frac{z}{L_n^0}\right)\left(\frac{l_n}{L_n^0}\right)}{\left(1 - \frac{z}{L_n^0}\right)}\right]. \quad (11)$$

Let $R_m^0 < x_m < R_{m+1}^0$ and $L_m^0 < y_m < L_{m+1}^0$, in which x_m and y_m are the positions of the sidelobe peaks in the starting pattern. Then

$$F_0(x_m) = \xi_m^0 \quad F_0(y_m) = \eta_m^0 \quad (12)$$

in which ξ_m^0 is the voltage level of the mth right-hand sidelobe and η_m^0 is the voltage level of the mth left-hand sidelobe in the starting pattern, with the main beam level normalized to unity.

Now let

$$F(x_m) = \xi_m \quad F(y_m) = \eta_m. \quad (13)$$

It follows that, if the perturbations r_n, l_n are small, then (13) approximately gives the heights of the mth right-hand and left-hand sidelobes in the *desired* pattern.

When (12) and (13) are substituted in (11), one obtains

$$\frac{\xi_m}{\xi_m^0} - 1 = \sum_{n=1}^{\bar{n}_R-1} \frac{\left(\frac{x_m}{R_n^0}\right)\left(\frac{r_n}{R_n^0}\right)}{\left(1 - \frac{x_m}{R_n^0}\right)} + \sum_{n=1}^{\bar{n}_L-1} \frac{\left(\frac{x_m}{L_n^0}\right)\left(\frac{l_n}{L_n^0}\right)}{\left(1 - \frac{x_m}{L_n^0}\right)} \quad (14)$$

$$\frac{\eta_m}{\eta_m^0} - 1 = \sum_{n=1}^{\bar{n}_R-1} \frac{\left(\frac{y_m}{R_n^0}\right)\left(\frac{r_n}{R_n^0}\right)}{\left(1 - \frac{y_m}{R_n^0}\right)} + \sum_{n=1}^{\bar{n}_L-1} \frac{\left(\frac{y_m}{L_n^0}\right)\left(\frac{l_n}{L_n^0}\right)}{\left(1 - \frac{y_m}{L_n^0}\right)}. \quad (15)$$

Equations (14) and (15) comprise the basis of the perturbation procedure. If one selects a starting pattern $F_0(z)$, the quantities R_n^0, L_n^0, ξ_m^0, η_m^0, x_m, and y_m are known. From the desired pattern, ξ_m and η_m are known. It follows that (14) and (15) constitute $(\bar{n}_R + \bar{n}_L - 2)$ simultaneous linear equations to solve for the perturbations r_n and l_n.

Once the r_n and l_n values are obtained, (7) and (8) can be used to determine R_n and L_n, which can then be inserted in $F(z)$ to determine a first approximation to the desired pattern. If this approximation is not adequate, the whole procedure can be repeated, with the newly found $F(z)$ playing the role of starting pattern. A series of iterations has been found to converge to the desired pattern for all practical cases which have been investigated. The rapidity of convergence depends on the complexity of the desired pattern and the appropriateness of the original $F_0(z)$ selected as the starting pattern. The number of iterations also depends on how closely one wishes to approximate the desired pattern.

Several examples will illustrate the design procedure.

Example 1

As a first demonstration of the design procedure, let it be desired to create a 30 dB sidelobe level Taylor pattern except that the second sidelobe to the right of the main beam is to be depressed to −40 dB.

We select $F_0(z)$ to be a conventional 30 dB Taylor pattern and choose $\bar{n}_R = \bar{n}_L = 8$. From [1, p. 23], it follows that $A_R^2 = A_L^2 = 1.74229$ and that $\sigma_R = \sigma_L = 1.05052$. Use of (5) gives the null positions in the starting pattern, listed in column 2 of Table I. When these null positions are used in (4), $F_0(z)$ is found to be the pattern displayed in Fig. 1(a). The sidelobe peak positions for this pattern are listed in column 3 of Table I.

Since the desired pattern $F(z)$ is to have sidelobes whose levels agree with those of $F_0(z)$ except for the second sidelobe on the right side, it follows that

$$\frac{\eta_m}{\eta_m^0} - 1 = 0, \quad \text{all } m$$

$$\frac{\xi_m}{\xi_m^0} - 1 = 0, \quad m \neq 2. \quad (16)$$

For $m = 2$, we have[1]

$$\xi_2 = 0.01 \quad \xi_2^0 = 0.0316 \quad \frac{\xi_2}{\xi_2^0} - 1 = -0.6835. \quad (17)$$

When the information contained in (16) and (17) is inserted in (14) and (15), together with the data from columns 2 and 3 of Table I, one obtains 14 simultaneous linear equations in the unknowns $(r_1/R_1^0), \cdots, (l_7/L_7^0)$. A computer solution gives the results listed in columns 4 and 5 of Table I. When these results are used in (7) and (8), the zeros of $F(z)$ are readily deduced. These zeros are found in columns 6 and 7 of Table I. Finally, if these zeros are used in (9), the pattern shown in Fig. 1(b) is obtained. Careful comparison of Figs. 1(a) and 1(b) shows that the levels of all sidelobes agree except for the first two to the right of the main beam. $F(z)$ as displayed in Fig. 1(b) is therefore the desired pattern except that the height of the first right-hand sidelobe is −31 dB when it should be −30 dB, and that the height of the second right-hand sidelobe is −37 dB when it should be −40 dB.

A second iteration, using Fig. 1(b) as the "starting" pattern results in Fig. 1(c). Now all sidelobes are within 0.25 dB of their desired heights. The main beam is slightly broadened (1.5 percent), consistent with having depressed a lobe, and the positions of the first and third lobes on the right side are shifted somewhat toward the second lobe, consistent with the primary result of having brought the second and third nulls closer together in order to depress the second sidelobe.

Example 2

As a further illustration of the design technique, let it be desired to create a symmetrical pattern with the three innermost sidelobes on each side of the main beam down −40 dB, the next four on each side down only −20 dB, and the far-out sidelobes tailing off as z^{-1}.

Once again we select $F_0(z)$ to be the conventional 30 dB Taylor pattern with $\bar{n} = 8$, shown in Fig. 1(a). The data of columns 2 and 3 of Table I apply, but now by symmetry

$$\frac{\eta_m}{\eta_m^0} - 1 = \frac{\xi_m}{\xi_m^0} - 1, \quad \text{all } m$$

$$\frac{l_n}{L_n^0} = \frac{r_n}{R_n^0}, \quad \text{all } m$$

[1] ξ_2^0 is actually slightly smaller than 0.0316, since the near-in Taylor sidelobes tail off slightly. Use of a more accurate value in the first iteration is unwarranted.

TABLE I

n	$R_n^0 = -L_n^0$	$x_n = -y_n$	r_n/R_n^0	l_n/L_n^0	R_n	L_n
1	1.483	1.791	0.0464	−0.0121	1.552	−1.465
2	2.099	2.534	0.0568	−0.0053	2.218	−2.088
3	2.970	3.450	−0.0401	−0.0032	2.851	−2.961
4	3.930	4.428	−0.0090	−0.0019	3.895	−3.922
5	4.927	5.434	−0.0038	−0.0012	4.908	−4.921
6	5.942	6.455	−0.0019	−0.0007	5.931	−5.938
7	6.968	7.484	−0.0008	−0.0004	6.962	−6.965
8	8.000					

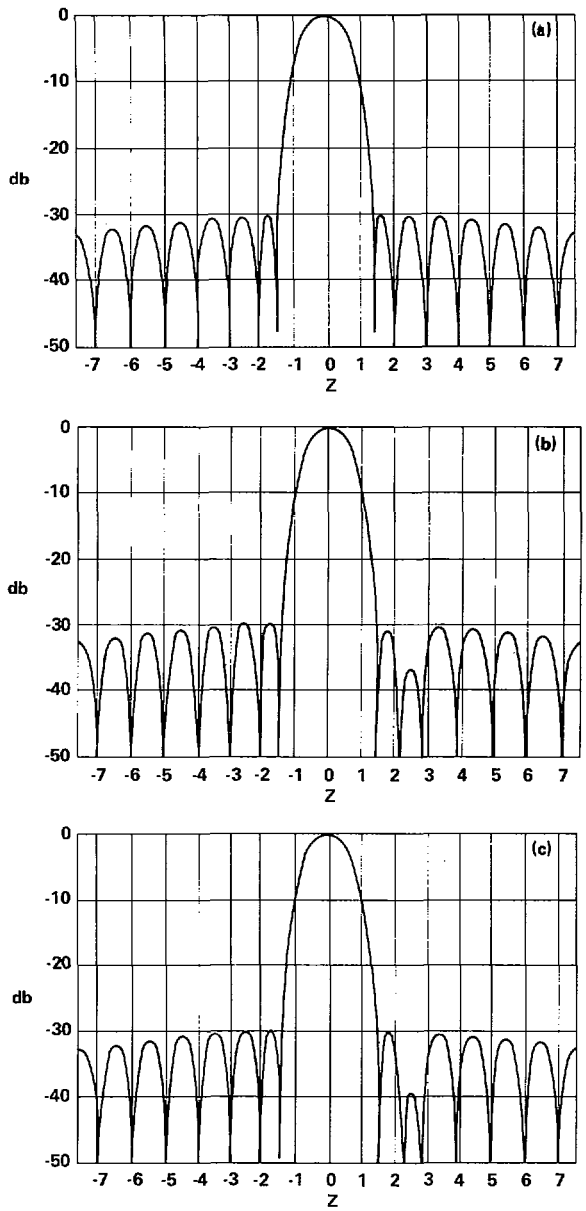

Fig. 1. Radiation patterns for Example 1. (a) Original 30 dB Taylor pattern. (b) First iteration. (c) Second iteration.

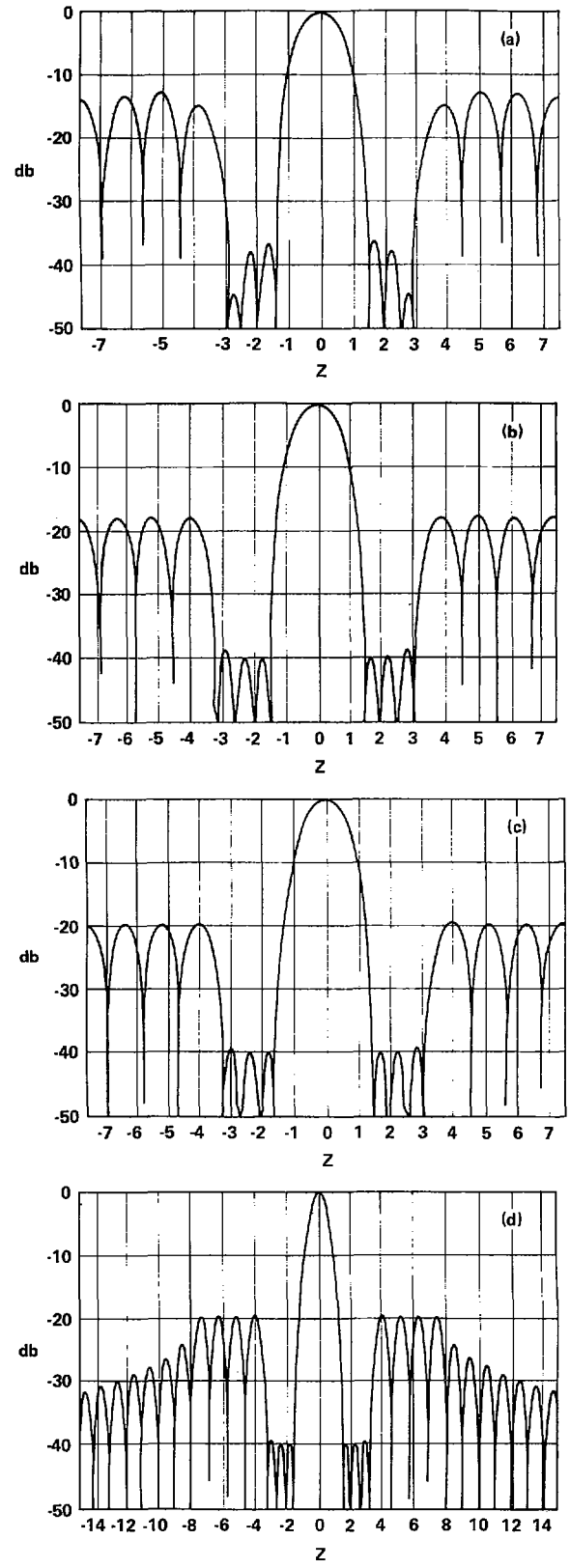

Fig. 2. Radiation patterns for Example 2. (a) First iteration. (b) Second iteration. (c) Third iteration. (d) Expanded range.

so that (15) is redundant and only (14) needs to be solved. Since $L_n^0 = -R_n^0$, (14) assumes the more compact form

$$\frac{\xi_m}{\xi_m^0} - 1 = \sum_{n=1}^{\bar{n}-1} \frac{2\left(\frac{x_m}{R_n^0}\right)^2 \left(\frac{r_n}{R_n^0}\right)}{1 - \left(\frac{x_m}{R_n^0}\right)^2}. \tag{18}$$

For this example,

$$\frac{\xi_1}{\xi_1^0} - 1 = \frac{\xi_2}{\xi_2^0} - 1 = \frac{\xi_3}{\xi_3^0} - 1 = -0.6835$$

$$\frac{\xi_4}{\xi_4^0} - 1 = \frac{\xi_5}{\xi_5^0} - 1 = \frac{\xi_6}{\xi_6^0} - 1 = \frac{\xi_7}{\xi_7^0} - 1 = 2.1623.$$

When this information is used in (18), a simultaneous solution gives r_n values which, when inserted in (7), give the zeros of the first iteration of $F(z)$. When these zeros are used in (1), the pattern of Fig. 2(a) results. One can observe overshoot on both the low sidelobes and the high sidelobes. A second iteration gives Fig. 2(b), and improvement is noted in the levels of all seven near-in sidelobes. A third iteration gives the pattern of Fig. 2(c), and now all seven sidelobes are within 0.5 dB of the desired values.

To show how the far-out sidelobes behave, Fig. 2(d) repeats Fig. 2(c) with the extent of the z scale doubled. A z^{-1} behavior is noted, in conformance with theory.

For the third iteration (Fig. 2(c)) the first zero occurs at $R_1 = 1.591$. Since $R_1^0 = 1.483$, it follows that $R_1/R_1^0 = 1.07$ and thus that there has been a seven percent broadening in the main beam. Apparently lowering the inner three sidelobes outweighed raising the remainder of the sidelobes in the effect on beamwidth.

Example 3

As a final illustration of the perturbation procedure, let it be desired to create an asymmetrical pattern with the seven innermost sidelobes on the right side at -25 dB, the seven innermost sidelobes on the left side at -15 dB, and the far-out sidelobes tailing off as z^{-1}.

This time we select $F_0(z)$ to be a conventional 20 dB Taylor pattern with $\bar{n} = 8$, depicted in Fig. 3(a). The first iteration gives the pattern shown in Fig. 3(b). The left-hand sidelobes average about 15 dB in height, but the innermost are too high and the outermost too low. The right-hand sidelobes average somewhat lower than 25 dB, although four of the lobes are quite close to design.

A second iteration is shown in Fig. 3(c). Now all seven sidelobes are within 1 dB of specification. Another iteration could have improved on this but was not undertaken. The main lobe is seen to be shifted to the right, as it should be, but to a position $z_0 = 0.3$, which is greater than the shift found using an earlier technique to create a 15/25 dB pattern [3]. This has been found to be entirely attributable to the fact that the earlier pattern was less asymmetric since it had close-in sidelobes which tailed off, whereas the present pattern has close-in sidelobes of a common height. The beam shift can be compensated for easily with the superposition of a small uniform phase progression.

Beamwidth comparisons are also interesting. The main beam in Fig. 3(c) is 8 percent narrower than the main beam in the comparable pattern found by the earlier technique [3]. This can be understood by noting that Fig. 3(c) has seven sidelobes of a common height on each side of the main beam (15 dB on the left, 25 dB on the right) whereas Fig. 2 of [3] shows a pattern in

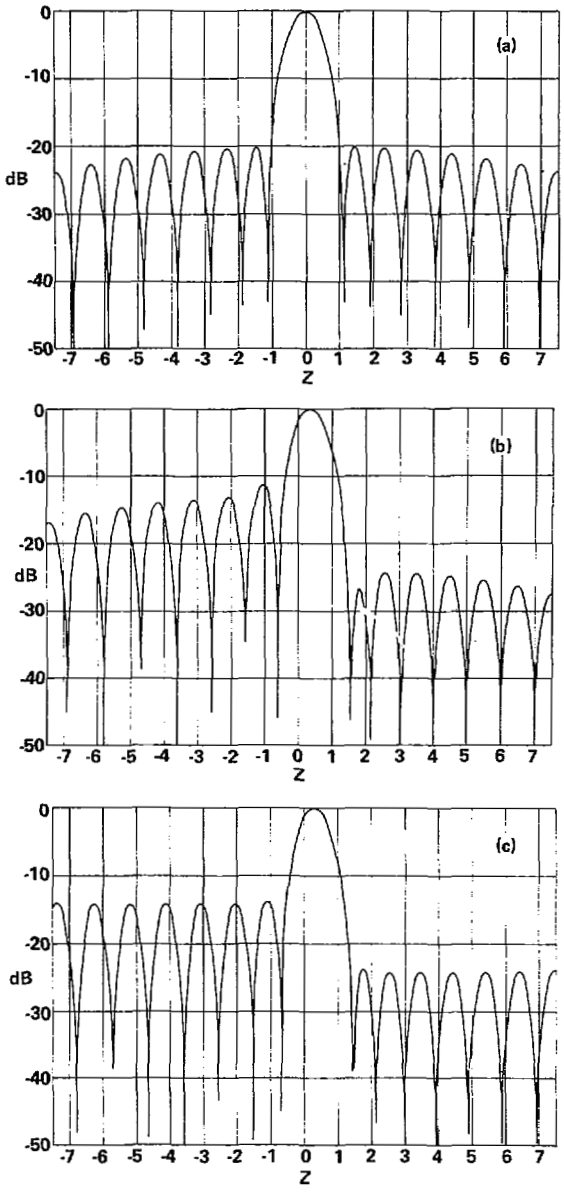

Fig. 3. Radiation patterns for Example 3. (a) Original 20 dB Taylor pattern. (b) First iteration. (c) Second iteration.

which the average height of the seven innermost left-hand sidelobes is 22 dB, and the average height of the seven innermost right-hand sidelobes is 26 dB.

Indeed, the beamwidth in Fig. 3(c) is even 5 percent narrower than the beamwidth in Fig. 3(a). This result seems reasonable, since one can argue that the beamwidth in Fig. 3(c) should be about the same as in a pattern in which the seven innermost sidelobes on both sides of the main beam are at a common height of 20 dB. However, such a pattern would have higher average sidelobes than the pattern of Fig. 3(a), and thus should have a narrower beamwidth.

Aperture Distribution

When the aperture distribution $f(p)$ is represented by a Fourier series, the transform of (9) is [3]

$$f(p) = \begin{cases} \frac{1}{2\pi} \sum_{m=-\bar{n}_L+1}^{\bar{n}_R-1} F(m)e^{-imp}, & p^2 \le \pi \\ 0, & p^2 > \pi \end{cases} \tag{21}$$

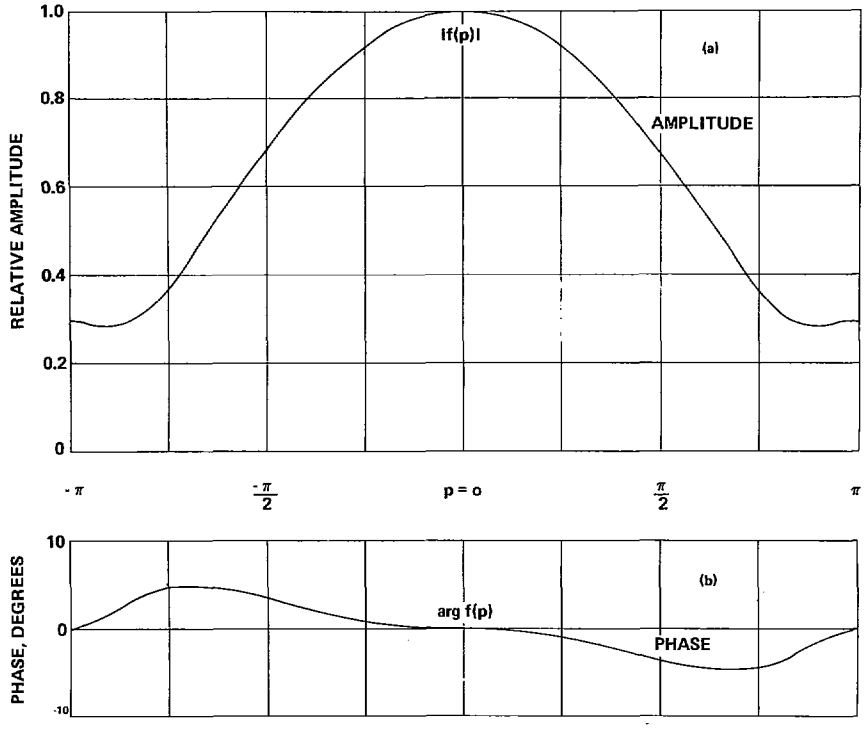

Fig. 4. Aperture distribution for pattern of Fig. 1(c).

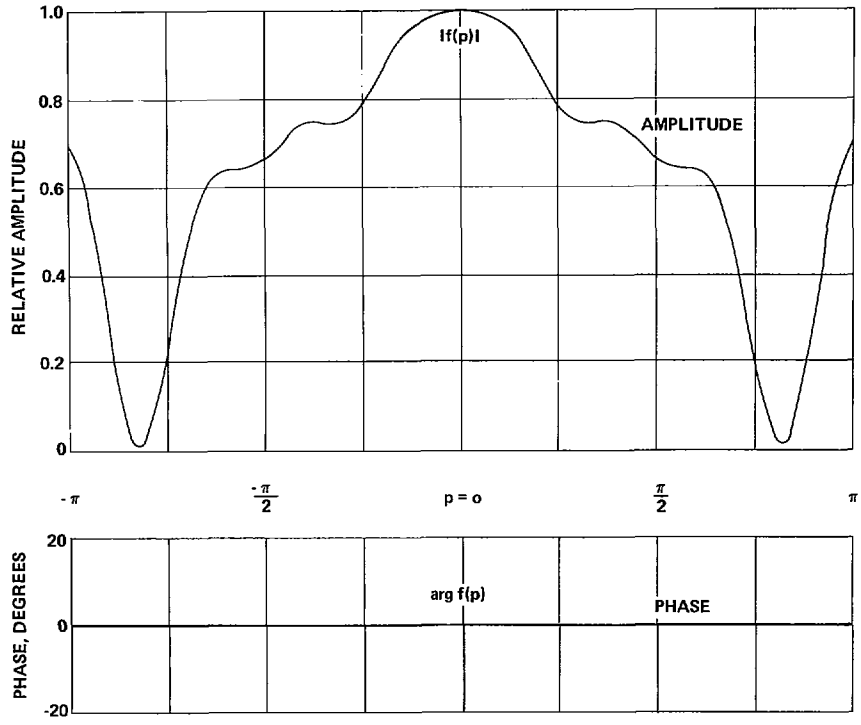

Fig. 5. Aperture distribution for pattern of Fig. 2(d).

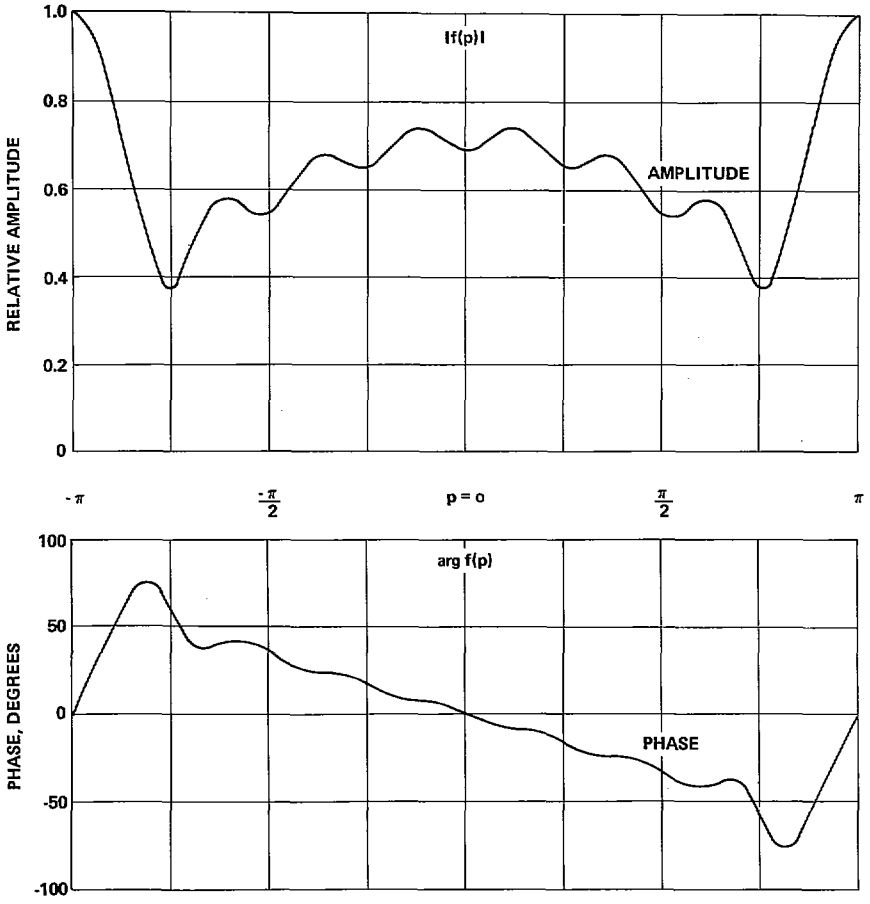

Fig. 6. Aperture distribution for pattern of Fig. 3(c).

in which m is an integer and $p = \pi x/a$ is the normalized aperture variable; the actual aperture runs from $x = -a$ to $x = +a$.

The computer printouts for $F(z)$ for each of the three illustrated examples whose patterns have been displayed in Figs. 1–3 were used to determine the values of $F(m)$ needed in (21). The results are shown in Figs. 4–6.

The amplitude and phase functions of the aperture distribution for Example 1 (30 dB Taylor except the second right-hand sidelobe is suppressed to −40 dB) are shown in Fig. 4. The aperture distribution (not shown) for the conventional 30 dB Taylor pattern has an amplitude function only slightly different from Fig. 4(a) and has a uniform phase function. The differences in the two distributions are listed in Table II.

It seems reasonable to argue that the two aperture distributions are comparably difficult to achieve. It follows that the patterns of Figs. 1(a) and 1(c) are also comparably difficult to achieve. However, the ability to obtain either at will and change from one to the other is a considerably more difficult proposition. Table II shows the percent change in amplitude and the change in phase needed to convert from one pattern to the other. It would be quite a challenge to the state of the art to attempt to control amplitude and phase in a discrete linear array within this tolerance level. Table II thus also sheds light on the tight tolerances needed for aperture distributions if one wishes to obtain very low sidelobe level patterns, and gives an indication of the size of the errors needed to affect a single sidelobe.

Fig. 5 displays the aperture distribution for Example 2 (three depressed lobes on each side of the main beam). Because of the pattern symmetry, this is an equiphase distribution. The amplitude variations are somewhat severe, but it would seem well within state of the art to construct a large linear array with the necessary tolerance to achieve this distribution.

Fig. 6 gives the aperture distribution for Example 3 (25 dB near-in sidelobes on one side, 15 dB on the other). This result should be contrasted to Fig. 3 of [3] which shows the aperture distribution for a 15/25 dB modified Taylor pattern. Fig. 6 indicates a similar phase variation, but with ripples, and with about five times the swing (±75° as opposed to ±15°). The amplitude distribution in Fig. 6 is strongly rippled and higher at the ends than in the middle, not at all like the smooth amplitude distribution for the 15/25 dB modified Taylor. The difference has been traced to the stringency of the uniform sidelobe level, as opposed to the declining level found in the modified Taylor.

Conclusions

A perturbation procedure has been developed which appears to be broadly applicable to the design of narrow beam low sidelobe level sum patterns from line sources with the important feature that the height of each individual sidelobe can be specified. The procedure involves starting with a factorable expression for a known pattern (such as a Taylor or Dolph–Chebyshev pattern), moving the zeros of this pattern in a controlled way, checking the outcome, and iterating until the desired pattern is approached to within a specified tolerance. In many widely different special cases which have been tried, convergence has been positive and

TABLE II
CHANGE IN APERTURE DISTRIBUTION NEEDED TO MODIFY A 30 dB TAYLOR PATTERN SO THAT THE SECOND RIGHT-HAND LOBE IS AT −40 dB

$p = \pi \frac{x}{a}$	Incremental Normalized Amplitude	Percent Change in Amplitude	Phase Change in Degrees
0	−0.0072	−2.39	0
$\frac{\pi}{12}$	−0.0120	−4.06	−0.1
$\frac{\pi}{6}$	−0.0187	−6.04	−0.4
$\frac{\pi}{4}$	−0.0175	−4.60	−0.8
$\frac{\pi}{3}$	−0.0096	−1.99	−1.5
$\frac{5\pi}{12}$	−0.0004	−0.07	−2.5
$\frac{\pi}{2}$	+0.0080	1.19	−3.4
$\frac{7\pi}{12}$	+0.0135	1.77	−4.3
$\frac{2\pi}{3}$	+0.0141	1.67	−4.8
$\frac{3\pi}{4}$	+0.0111	1.22	−4.7
$\frac{5\pi}{6}$	+0.0064	0.67	−3.4
$\frac{11\pi}{12}$	+0.0035	0.35	−1.3
π	0	0	0

rapid. The corresponding aperture distributions can be found routinely and computer costs are extremely reasonable.

Perhaps one of the most fruitful areas of application of this perturbation technique is diagnostics. It is now possible to take an experimental pattern (providing it has deep nulls) and analyze why it does not achieve the design goal merely by perturbing the design pattern until it is transformed to the experimental pattern. The resulting aperture distribution, when compared to the design aperture distribution, reveals exactly what changes need to be made in aperture excitation in order to correct the experimental pattern.

ACKNOWLEDGMENT

The author is once again indebted to Ralph M. Johnson who did all the computer programming in this study.

REFERENCES

[1] C. L. Dolph, "A current distribution for broadside arrays which optimizes the relationship between beamwidth and side-lobe level," *Proc. IRE*, vol. 34, pp. 335–348, June 1946.
[2] T. T. Taylor, "Design of line-source antennas for narrow beamwidth and low side lobes," *IRE Trans. Antennas Propagat.*, vol. AP-3, pp. 16–28, Jan. 1955.
[3] R. S. Elliott, "Design of line-source antennas for narrow beamwidth and asymmetric low sidelobes," *IEEE Trans. Antennas Propagat.*, vol. AP-23, pp. 100–107, Jan. 1975.
[4] R. F. Hyneman, "A technique for the synethesis of line-source antenna patterns having specified sidelobe behavior," *IEEE Trans. Antennas Propagat.*, vol. AP-16, pp. 430–435, July 1968.
[5] W. L. Stutzman, "Sidelobe control of antenna patterns," *IEEE Trans. Antennas Propagat.* (Commun.), vol. AP-20, pp. 102–104, Jan. 1972.

Efficient Numerical Techniques for Solving Pocklington's Equation and Their Relationships to Other Methods

DONALD R. WILTON, MEMBER, IEEE, AND CHALMERS M. BUTLER, MEMBER, IEEE

***Abstract*—It is shown that testing Pocklington's equation with piecewise sinusoidal functions yields an integro-difference equation whose numerical solution is identical to that of the point-matched Hallen's equation when a common set of basis functions is used with each. For any choice of basis functions, the integro-difference equation has the simple kernel, the fast convergence, the simplicity of point-matching, and the adequate treatment of rapidly varying incident fields, but none of the additional unknowns normally associated with Hallen's equation. Furthermore, for the special choice of piecewise sinusoids as the basis functions, the method reduces to Richmond's piecewise sinusoidal reaction matching technique, or Galerkin's method. It is also shown that testing with piecewise linear (triangle) functions yields an integro-difference equation whose solution converges asymptotically at the same rate as that of Hallen's equation. The resulting equation is essentially that obtained by approximating the second derivative in Pocklington's equation by its finite difference equivalent. The authors suggest a simple and highly efficient method for solving Pocklington's equation. This approach is contrasted to the point-matched solution of Pocklington's equation and the reasons for the poor convergence of the latter are examined.**

INTRODUCTION

In order to handle complicated problems using moment methods it is necessary to optimize numerical solution procedures from the point of view of speed and convergence. This leads one to a study of the properties of various integral equation formulations and of the choice of basis and testing functions [1] in solution methods, both with an end toward improving the numerical efficiency of given computations. Also desirable are techniques which are conceptually simple to apply (so as to minimize programming time) and which have a wide range of applicability.

One difficulty which frequently arises in the numerical solution of an integral equation is the appearance of derivatives outside the vector potential integrals on the induced currents. For thin wires, this problem, encountered in Pocklington's equation, is usually handled in one of three ways. First, the E-field integro-differential equation may be converted to a Hallen type equation plus boundary conditions on the current. This procedure has the disadvantages of introducing additional unknowns into the problem (associated with the homogeneous solutions of the differential operator) and of producing a new integral equation which does not incorporate the boundary conditions on the unknown current. However, the Hallen-type equation offers good convergence for almost all commonly used basis functions. In the second scheme, the kernel of the E-field integral equation is made regular by approximations which result in the so-called reduced kernel, and the differentiation is brought inside the integral and onto the unknown current by integration by parts. When collocation (point-matching) is used with this technique and a basis representation for current is chosen which permits slope discontinuities in current, e.g., piecewise constant or piecewise linear representation, convergence is relatively slow.

Manuscript received October 7, 1974; revised July 6, 1975. This work was supported in part by the National Science Foundation under Grant GU-3833.
The authors are with the School of Engineering, University of Mississippi, University, MS 38677.